



## From nanowires to cubes of CdO: Ethanol gas response

A.S. Kamble<sup>a</sup>, R.C. Pawar<sup>a</sup>, J.Y. Patil<sup>b</sup>, S.S. Suryavanshi<sup>b</sup>, P.S. Patil<sup>a,\*</sup>

<sup>a</sup> Thin Films Materials laboratory, Department of Physics, Shivaji University, Kolhapur 416004, Maharashtra, India

<sup>b</sup> Ferrite Materials Laboratory, School of Physical Sciences, Solapur University, Solapur, Maharashtra, India

### ARTICLE INFO

#### Article history:

Received 5 August 2010

Received in revised form

22 September 2010

Accepted 26 September 2010

#### Keywords:

Cadmium oxide

Gas sensing properties

Chemical bath deposition

### ABSTRACT

The cadmium oxide (CdO) thin films have been synthesized by chemical bath deposition (CBD) method from an aqueous cadmium acetate solution for different time periods. The effect of film thickness on structural, morphological and wettability properties have been investigated by means of X-ray diffraction (XRD), scanning electron microscopy (SEM) and contact angle measurements. The chemically deposited CdO thin films were polycrystalline with face centered cubic crystal structure. The average crystallite size was found to be in the range of 28–31 nm. An interesting morphological transition from nanowires to microcubes was observed with change in deposition time from 25 to 100 h at room temperature. The deposited CdO films exhibit excellent sensing properties against ethanol at 673 K. The 0.8239  $\mu\text{m}$  thick films comprising nanowires deposited for 75 h showed the better ethanol gas performance as compared to other films.

© 2010 Elsevier B.V. All rights reserved.

### 1. Introduction

Semiconductor metal oxide based gas sensors have attracted great attention over several decades due to their unique advantages, such as high sensitivity, low cost, ease of fabrication and good compatibility to silicon micro-fabrication [1–3]. The gas sensing properties of metal oxide depends naturally on their catalytic or surface morphological features [4], such as grain size [5], porosity and thickness [6]. Various semiconductors such as SnO<sub>2</sub>, TiO<sub>2</sub>, WO<sub>3</sub>, In<sub>2</sub>O<sub>3</sub>, Ga<sub>2</sub>O<sub>3</sub>, ZnO and CdO are used as sensing elements of gas sensors. However, these materials are still not as selective as one would expect, since they also sense other gases. In addition the stability of some of the materials is not very good, resulting in poor reliability due to aging and humidity induced effects. Among the aforementioned oxides, CdO has received less attention due to narrow energy band gap [7]. However, CdO film shows higher mobility value, which is necessary for high conductivity transparent conducting oxide materials especially when low free carrier absorbance is desired [8].

Several methods have been employed for synthesizing CdO nanowires in the literature, including spray pyrolysis [9], electrochemical deposition [10], metal-organic vapor phase epitaxy [11], and rf sputtering [12]. However, these techniques are energy consumable and involve high temperature process. In order to tackle these problems CBD is the most promising method to deposit CdO

thin films at room temperature. It is one of the single step solution phase method useful for the preparation of compound semiconductors from aqueous solutions. It is also known as controlled precipitation and solution deposition method, and widely used for the large area deposition. It allows us to easily control the growth factors such as film thickness, deposition rate and crystalline quality by varying the solution pH, growth temperature and bath concentration. The low temperature deposition avoids oxidation and corrosion of metallic substrates and various substrates including insulators, semiconductors and metals can be used for deposition.

To the best of our knowledge there are reports on preparation and characterization of CdO nanowires using CdSO<sub>4</sub> and CdCl<sub>2</sub> as source materials of Cd ion [13,14]. No attempt has been made to deposit them using cadmium acetate as a source of Cd ions in an aqueous alkaline bath. In the present work CdO thin films are chemically deposited via acetate medium using CBD method. The ammonium acetate formed in course of reaction act as buffer to maintain prescribed pH value over whole deposition period. The deposition is carried out for different time periods in order to get terminal thickness. The maximum thickness 1.01  $\mu\text{m}$  is observed for 100 h. Further, the effect of thickness on structural, morphological and wettability properties has been investigated. The gas sensing performance of the films has been evaluated in terms of gas concentration and operating temperature.

### 2. Experimental details

Before the deposition of CdO thin films, glass slides were cleaned with detergent and distilled water, then boiled in chromic acid (0.5 M) for 15 min, then slides washed with double distilled water and further ultrasonicated for 15 min. Finally the substrates were degreased in AR grade acetone and used for deposition.

\* Corresponding author. Tel.: +91 231 2609229; fax: +91 231 2691533.

E-mail addresses: [psp.phy@unishivaji.ac.in](mailto:psp.phy@unishivaji.ac.in), [pravinshinde.physics@yahoo.com](mailto:pravinshinde.physics@yahoo.com) (P.S. Patil).

CdO thin films were deposited by a CBD method, which consisted of an alkaline cadmium solution containing glass substrates immersed in it. 0.1 M cadmium acetate  $\text{Cd}(\text{CH}_3\text{COO})_2$  was used as a source of cadmium and to make it alkaline an aqueous ammonia solution was added with constant stirring. Initially the solution becomes milky turbid due to the formation of  $\text{Cd}(\text{OH})_2$ . Turbidity vanishes after further addition of excess ammonia and solution became clear and transparent. The pH of resultant solution was  $\sim 12$ . The substrates were immersed in the bath at room temperature without stirring. After about 10 h the solution becomes turbid and precipitation starts. During the precipitation heterogeneous reaction occurred and the deposition of  $\text{Cd}(\text{OH})_2$  takes place on the substrate. The films prepared by this method are uniform and well adherent to the substrates. The deposited films were removed after different time intervals of 25, 50, 75 and 100 h and rinsed in distilled water. The films are denoted as C25, C50, C75 and C100. All these films are subsequently annealed at 723 K for the removal of water and any other impurities.

The thickness of these films was measured using AMBIOS Make XP-1 model. The phase formation and crystallinity were analyzed by X-ray diffractometer (XRD, Philips PW-3710 Cr  $K\alpha$  line). The surface morphology of the films was observed using SEM (model JEOL-JSM 6360). Contact angle measurement was carried out on Rame-Hart USA equipment with CCD camera.

The two probe technique was used to measure the electrical resistance in air and in presence of ethanol gas [15]. For electrical measurements the Ohmic contacts were made with the help of silver paste to form sensing elements. The gas sensing studies were carried out on these sensing elements in static gas chamber to sense the ethanol in air ambient. The sensing element was kept directly on heater in the gas chamber and the temperature was varied from 473 to 723 K. The temperature of the sensing element was monitored by chromel–alumel thermocouple placed in contact with the sensor. The known volume of the ethanol was introduced in to the gas chamber pre-filled with air and it was maintained at atmospheric pressure. The electric resistance of the sensing element was measured before and after exposure to ethanol gas using a sensitive digital multimeter (Hawlette packard). The sensitivity ( $s$ ) of the sensing element is defined as

$$\%S = \left( \frac{R_a - R_g}{R_a} \right) \times 100$$

where  $R_a$  and  $R_g$  are the resistance values of the sensor element in air and in presence of ethanol.

### 3. Reaction and growth mechanism

In CBD the formation of solid phase from solution takes place in two steps as nucleation and particle growth [14]. The positively charged and anisotropic cadmium hydroxide nuclei are produced on the substrate when ionic product starts to exceed the solubility product; such nuclei assemble together to form nanostrand structure with high aspect ratio.

The chemical reaction culminating the formation of  $\text{Cd}(\text{OH})_2$  is written as



where  $\text{Cd}^{2+}$  in the chemical bath provided by the dissociation of  $\text{Cd}(\text{CH}_3\text{COO})$  and  $\text{OH}^-$  ions are released by the dissociation of  $\text{NH}_4\text{OH}$ . The surface of nanostrand is positive and thermodynamically unstable. Further, these nanostrands act as building block to form nanowires on increase in ionic product of growth solution. The agglomeration of nanowires takes place to form cube like morphology when such a deposition is carried out for longer period. When as-deposited films were heated at 723 K in air,  $\text{Cd}(\text{OH})_2$  is converted into CdO phase. A chemical reaction given below explains the oxide formation [14].



### 4. Thickness measurements

The films deposited for various time periods were smooth, brown in color and uniformly covering the substrate with good adherence. The thickness of these films was measured using AMBIOS Make XP-1 model of surface profiler with 1 Å vertical resolution. Fig. 1 shows the variation of film thickness with deposition time. It is observed that the film thickness goes on increasing with deposition time up to 100 h and after that becomes saturated. The

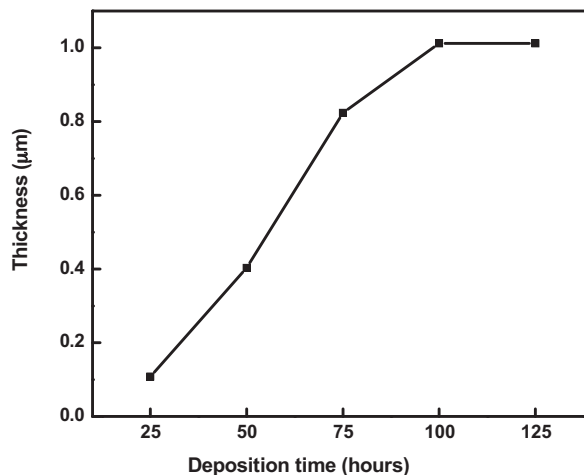


Fig. 1. Variation of thickness of CdO thin films with deposition time.

film thickness was increased from 0.1079  $\mu\text{m}$  to 1.0124  $\mu\text{m}$  for 25 h to 100 h, respectively.

### 5. X-ray diffraction studies

Fig. 2 shows XRD patterns of C25, C50, C75 and C100 CdO films. The diffraction peaks show the formation of polycrystalline nature with a face centered cubic crystal structure. The observed 'd' values of the films are in good agreement with those reported in the JCPDS (73-2245) for CdO. Films exhibit characteristic peaks along (1 1 1), (2 0 0), (2 2 0) planes. The peak intensity of (1 1 1) plane was relatively higher than the other reflections. The increment in the peak intensities for all the planes indicates the improvement in crystallinity of the CdO with increase in thickness. The crystallite size was estimated using Debye Scherrer's formula;  $t = 0.9\lambda / \beta \cos \theta$  where  $\lambda$  is X-ray wavelength,  $\theta$  is the Bragg's angle and  $\beta$  is the full width of diffraction line (FWHM) at the half of maximum intensity. The calculated average crystallite size is in the range of 28–31 nm.

### 6. Surface morphological studies

The two dimensional surface morphological studies of the annealed CdO thin films C25, C50, C75 and C100 have been carried out from SEM. Fig. 3(a) and (b) shows the SEM images of C25 and C50 films respectively, from these micrographs one can see that

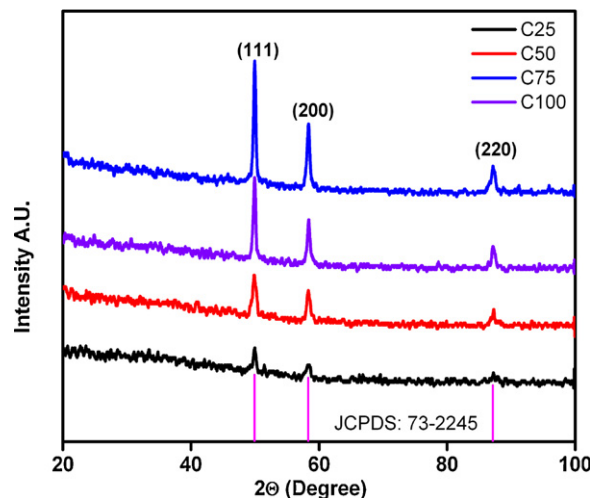


Fig. 2. XRD patterns of the CdO films for different thicknesses.

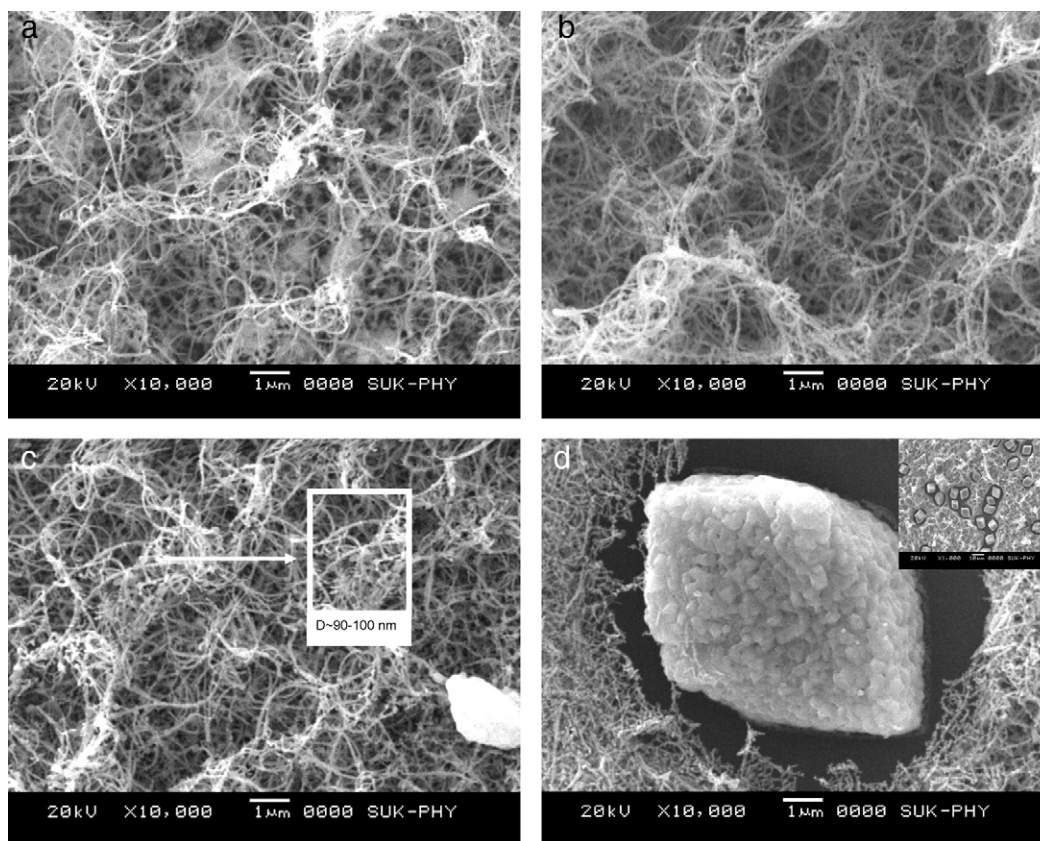


Fig. 3. SEM micrographs of (a) C25, (b) C50, (c) C75, and (d) C100 films at 10,000 $\times$  magnification. Inset (d) shows 20–30% conversion of nanowires to cubes.

total coverage of the substrate with the randomly distributed CdO nanowires having diameter of about 90–100 nm and length ranging up to several tens of micrometers. Fig. 3(c) shows the SEM image of C75 film. It is observed that agglomeration of nanowires to cubes is just started with a very small amount of reduction in effective surface area. The whole substrate is covered with nanowires and few percentage of small cubes. However Fig. 3(d) of C100 film depicts the agglomeration of nanowires to cubes with the large amount of reduction in effective surface area. Inset shows the low magnified SEM image revealing 20–30% conversion of nanowires to cubes.

## 7. Wettability study

The wetting property of a surface is defined according to the contact angle ( $\theta$ ), which forms a liquid droplet on the three phases contact line (interface of three media – air, water and film surface). A surface is regarded as wetting when the contact angle, which forms a drop with this one, is lower than 90°. In the opposite case (the contact angle is higher than 90°), the surface is nonwetting. For water, the terms “hydrophilic” and “hydrophobic” are commonly used for wetting and nonwetting surfaces respectively. The contact angle is expected to depend upon local inhomogeneity, chemical composition and the surface roughness. It is known that the hydrophilic nature is an essential factor for better performance in various applications such as gas sensors, photo electrochemical cells, super capacitors, etc. [16,17]. Fig. 4 illustrates the variation of contact angle with thickness of the film. It is found that all surfaces are hydrophilic in nature as water Contact angle is less than 90°. Contact angle is found to be decreased with increase in film thickness due to improvement in roughness and network-like architecture, which creates air crevices in-between the wires and also the thick film has relatively less internal and external strain

energies compared to the thin one [18]. Variation in thickness, surface roughness and hence in contact angle with thickness is given in Table 1. The lowest contact angle 18° is observed for C100 film and the highest one 45° for the C25 film. The film C75 is more hydrophilic as compared with C50 film, which is favorable for gas adsorption.

## 8. Gas sensing characteristics

In ethanol gas sensing oxygen sorption plays an important role in electrical transport properties of CdO thin film. The oxygen sorption removes the conduction electrons and they lower the conductance of CdO. When the CdO film is surrounded by air, oxygen molecules adsorbs on the surface to generate chemisorbed

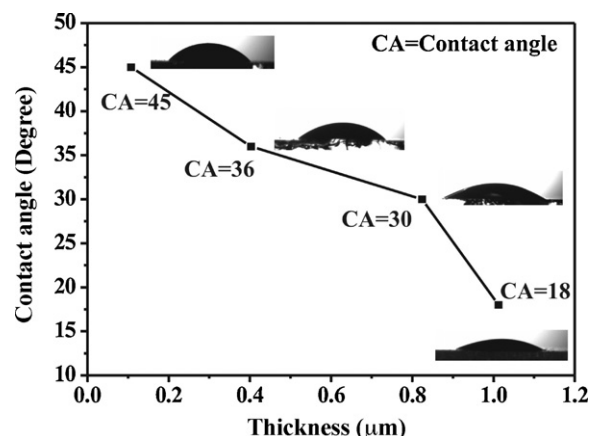


Fig. 4. Variation in contact angle with the film thickness.



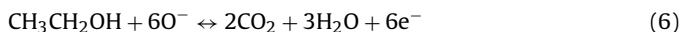
**Table 1**  
The values of response time, recovery time and roughness.

Film code	Thickness ( $\mu\text{m}$ )	Rough-ness ( $\text{\AA}$ )	Contact angle ( $^\circ$ )	% Sensitivity	Response time in (s)	Recovery time in (s)
C25	0.1079	398	45	15.30	48	171
C50	0.4030	1114	36	31.30	43	193
C75	0.8239	3396	30	38.16	31	186
C100	1.0124	5125	18	33.95	39	180

oxygen species ( $\text{O}_2^-$ ,  $\text{O}^{2-}$  and  $\text{O}^-$ ) by capturing electrons from conduction band. Thus CdO thin film will become highly resistive. When ethanol gas is introduced, the CdO exposed to the traces of reductive gas. By reacting with oxygen species on the CdO film surface the reductive gas will reduce the concentration of oxygen species on the film surface and thus increase the electron concentration. As a result the CdO thin film should become more conductive. Hence the sensing mechanism of CdO to ethanol gas may be described as follows. First reactive oxygen species such as  $\text{O}_2^-$ ,  $\text{O}^{2-}$  and  $\text{O}^-$  are adsorbed on the CdO surface at elevated temperature. It should be noted that chemisorbed oxygen species depend strongly on temperature. At low temperatures  $\text{O}_2^-$  is commonly chemisorbed. At high temperatures however  $\text{O}^-$  and  $\text{O}^{2-}$  are commonly chemisorbed, while  $\text{O}_2^-$  disappear rapidly [19]. The reaction kinematics can be described as follows [20].



Thus, the conductance of CdO thin film increases as the ethanol gas is introduced in to the test chamber due to exchange of electrons between ionosorbed species and CdO thin film. The reaction between ethanol and ionic oxygen species can be described as [21]



### 8.1. Effect of thickness and morphological conversion on the gas response

Fig. 5 shows the sensitivity as a function of operating temperature for C25, C50, C75 and C100 films under the exposure of 1000 ppm ethanol gas. It is seen that, at the same ethanol gas concentration, the CdO sensor shows different responses for different films. The ethanol gas response is higher at an optimum operating temperature ( $T_{\text{OP}}$ ) of the film and it is lower on either side of  $T_{\text{OP}}$ . The observed value of  $T_{\text{OP}}$  for all films is 673 K. However, the maximum gas sensitivity 38.13% is observed for C75 film as compared to the

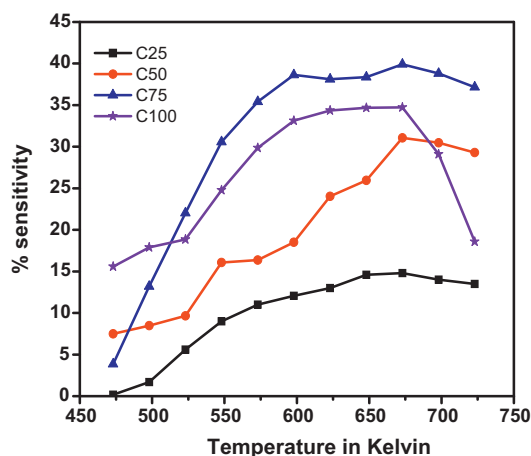


**Fig. 5.** Gas response for all the films as a function of operating temperature at 1000 ppm ethanol gas.

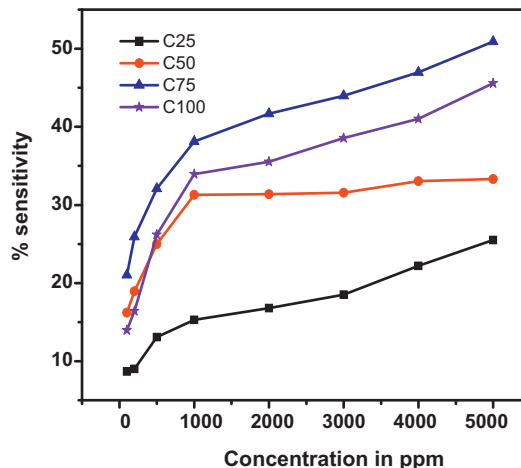


**Fig. 6.** Variation of % sensitivity as a function of thickness.

C25 (15.30%), C50 (31.30%) and C100 (33.95%) films. The change in gas sensitivity is attributed to the variation in effective surface area. It is well known that the sensitivity of the metal-oxide semiconductor sensors is mainly determined by the interactions between the target gas and the surface of the sensors. So, it is obvious that for the greater surface area of the materials, the interaction between the adsorbed gases and the sensor surface are stronger, i.e. gas sensitivity is higher [22]. In the present case, the careful observation of SEM images of C25, C50, C75 and C100 films indicate that the film C25 and C50 have relatively smooth surface, which offered low effective surface area for interaction with gas molecules. Also, the C25 and C50 films have lower thickness (see Table 1). On contrary, the film C75 has the dispersed nanowires like morphology with almost same diameter, and increased film thickness than C50 and C25, which assists in improving effective surface area to interact with gas molecules. The film C75 exhibits very less amount of small cubes on the surface, indicating initiation of nanowires to cubes conversion. The increased roughness and hydrophilicity causes it to become more favorable for gas adsorption. Thus, although the few percentage of small sized cube conversion is observed, the resultant effect of increased effective surface area and hydrophilicity causes it to give higher gas sensitivity compared with C50. However in case of C100 film, 20–30% micro cube like morphology is formed due to the agglomeration of nanowires. This nanowire conversion reduces the large amount of effective surface area, which results the lower gas sensitivity. Fig. 6 shows the response of a CdO films as a function of ethanol gas concentration at 673 K. It is revealed that response increases almost linear for all the films as concentration is increased from 100 to 1000 ppm afterwards there is a slow increase in response with concentration.

Fig. 7 shows the variation in gas sensitivity with respect to thickness. It is observe that initially the sensitivity increases as the film thickness increases up to certain thickness and afterwards it starts to decrease with increasing thickness. The results are in good agreement with the literature [9,23]. The dynamic variation in sensitivity of films C25, C50, C75 and C100 with operating temperature at 673 K for the exposure of 1000 ppm ethanol gas is shown in Fig. 8.

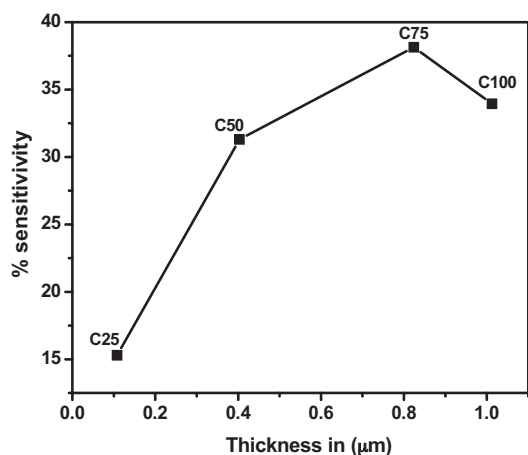


Fig. 7. Sensing characteristics of the CdO films as a function of ethanol concentration in air at 673 K.

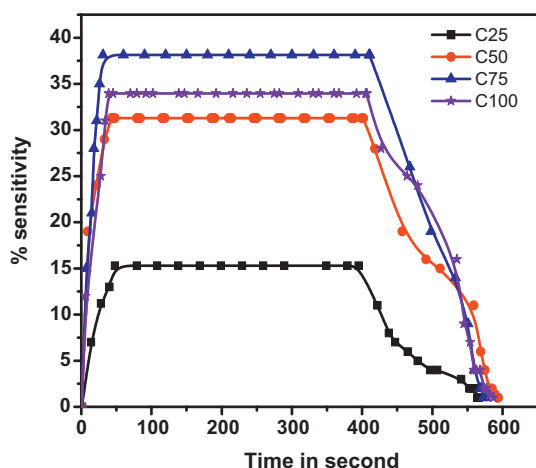


Fig. 8. The dynamic variation of sensitivity of films C25, C50, C75 and C100 with time at operating temperature 673 K for the exposure of 1000 ppm ethanol gas.

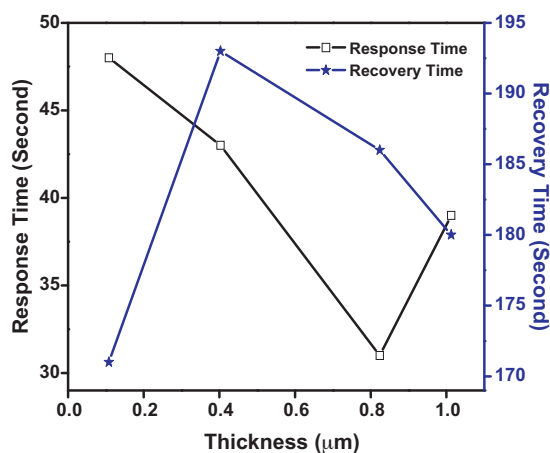


Fig. 9. Variation of response and recovery time with thickness.

All the films show the fast gas response when gas introduced in the gas chamber and it comes nearly at same value after gas pumping away from the chamber. The response and recovery times for different thicknesses of CdO films, operated at 673 K under the exposure of 1000 ppm ethanol gas are given in Fig. 9. The film C75 having better performance possesses the response and recovery time as 30 s and 186 s respectively. All the values of gas sensing response for different thicknesses are given in Table 1.

## 9. Conclusions

Polycrystalline CdO thin films with different thicknesses with cubic crystal structure have been successfully deposited by CBD method. The SEM image reveals the formation of CdO nanowires and microcubes, with respect to the deposition time. The sensing properties were studied at 1000 ppm concentrations of ethanol. The higher ethanol response of about 38.13% is observed for porous CdO nanowires with a 0.8239 μm film thickness and above this the response is decreased with increase in thickness, which is attributed to decrement in effective surface area.

## Acknowledgement

Authors are thankful to University Grants Commission (UGC) for financial support under the DRS-SAP-II and UGC-ASIST programme.

## References

- [1] A.S. Zuruhi, A. Kolmalov, N.C. Macdonald, M. Moskovits, *Appl. Phys. Lett.* 88 (2006) 1029041.
- [2] Y.S. Kim, S.C. Ha, K. Kim, H. Yang, J.T. Park, C.H. Lee, J. Choi, J. Paek, K. Lee, *Appl. Phys. Lett.* 86 (2005) 2131051.
- [3] H. Huang, O.K. Tan, Y.C. Lee, T.D. Tran, M.S. Tse, X. YaO, *Appl. Phys. Lett.* 87 (2005) 1631231.
- [4] E. Shomni, *Anal. Chim. Acta* 568 (2006) 28.
- [5] S. Shukla, P. Zhang, H.J. Cho, S. Seal, L. Ludwig, *Sens. Actuators B* 120 (2007) 573.
- [6] S. Chrioulakis, M. Suche, E. Koudoumas, M. Katharakis, N. Katharakis, M. Katsarakis, G. Kiriakidis, *Appl. Surf. Sci.* 252 (2006) 5351.
- [7] D.M.C. Galicia, R.C. Perez, O.J. Sandoval, S.J. Sandoval, G.T. Delgado, C.I.Z. Romero, *Thin Solid Films* 371 (2000) 105.
- [8] J.S. Cruz, G.T. Delgado, R.C. Perez, S.J. Sandoval, O.J. Sandoval, C.I.Z. Romero, J.M. Marin, O.Z. Angel, *Thin Solid Films* 493 (2005) 83.
- [9] R.R. Salunkhe, D.S. Dhawale, D.P. Dubal, C.D. Lokhande, *Sens. Actuators B: Chem.* 140 (2009) 86.
- [10] Y.W. Wang, C.H. Liang, G.Z. Wang, T. Gao, S.X. Wang, J.C. Fan, L.D. Zhang, *J. Mater. Sci. Lett.* 20 (2001) 1687.
- [11] D. Lamb, S.J.C. Irvine, *Thin Solid Films* 518 (2009) 1222.
- [12] B. Saha, S. Das, K.K. Chattopadhyay, *Sol. Energy Mater. Sol. Cells* 91 (2007) 1692.
- [13] V.R. Shinde, H.-S. Shim, T.P. Gujar, H.J. Kim, W.B. Kim, *Adv. Mater.* 20 (2008) 1008.
- [14] D.S. Dhawale, A.M. More, S.S. Latthe, K.Y. Rajpure, C.D. Lokhande, *Appl. Surf. Sci.* 254 (2008) 3269.
- [15] R.C. Pawar, J.S. Shaikh, A.V. Moholkar, S.M. Pawar, J.H. Kim, J.Y. Patil, S.S. Suryavanshi, P.S. Patil, *Sens. Actuators B: Chem.* (in press).
- [16] R.S. Mane, J. Chang, D. Ham, B.N. Pawar, T. Ganesh, B.W. Cho, J.K. Lee, S.-H. Han, *Curr. Appl. Phys.* 9 (2009) 87.
- [17] X. Xu, J. Wang, Y. Long, *Sensors* 6 (2006) 1751.
- [18] V. Vonk, S.J. van Reeuwijk, J.M. Dekkers, S. Harkema, A.J.H.M. Rijnders, H. Graafsm, *Thin Solid Films* 449 (2004) 133.
- [19] J. Cerdá Belmonte, J. Manzano, J. Arbiol, A. Cirera, J. Puigcorbe, A. Vila, N. Sabate, I. Gracia, C. Cane, J.R. Morante, *Sens. Actuators B: Chem.* 114 (2006) 881.
- [20] P.P. Sahay, *J. Mater. Sci.* 40 (2005) 4383.
- [21] T. Gao, T.H. Wang, *Appl. Phys. A* 80 (2005) 1451.
- [22] J.F. Chang, H.H. Kuo, I.C. Leu, M.H. Hon, *Sens. Actuators B: Chem.* 84 (2002) 258.
- [23] V.R. Shinde, T.P. Gujar, C.D. Lokhande, R.S. Mane, S.H. Han, *Mat. Sci. Eng. B* 137 (2007) 119.